Dual Band Kinetic Inductance Bolometers for Submillimeter-wave Imaging Experimental and Theoretical Optical Response

Dabironezare, S.O.; Hassel, J.; Gandini, E.; Grönberg, L.; Sipola, H.; Vesterinen , V.; Llombart, N.

DOI
10.1109/IRMMW-THz.2018.8509946

Publication date
2018

Document Version
Final published version

Published in
43rd International Conference on Infrared, Millimeter, and Terahertz Waves, IRMMW-THz 2018

Dual Band Kinetic Inductance Bolometers for Submillimeter-wave Imaging: Experimental and Theoretical Optical Response

S.O. Dabironezare[1], J. Hassel[2], E. Gandini[1], L. Grönberg[2], H. Sipola[2], V. Vesterinen[2], and N. Llombart[1]
[1] Terahertz Sensing Group, Delft University of Technology, Delft, the Netherlands
[2] VTT Technical Research Center of Finland, Helsinki, Finland

***Abstract*—In this contribution, a focal plane array (FPA) at sub-millimeter wavelengths is presented for security applications. The detectors are based on kinetic inductance bolometers. Two frequency selective absorber (FSA) sets were designed to implement a security imager. The effective pattern of the imager coupled to a black body point source over a wide frequency band (1:6) was demonstrated experimentally with excellent agreement to the one estimated by using a Fourier optics based technique.**

I. INTRODUCTION

The next generation of THz imagers for stand-off detection of concealed weapons require the acquisition of images as large as a human body, ≥ 100000 pixels, and at high frame rates, ≥ 10 Hz [1]. The architecture of such imagers is typically composed of a quasi-optical component coupled to a focal plane array (FPA). A large format FPA leads to longer integration time comparable to the frame rate which relaxes the sensitivity requirement of such FPAs.

Kinetic inductance detectors (KIDs) [2] are used for implementing large number of detectors in the order of several thousand at sub-millimeter wavelengths. Bolometer based KIDs provide the possibility of having large FPAs with medium cooled temperature and a reasonable cost for passive imaging. Exploiting this technology, a dual band FPA suited for future security applications was designed, Fig. 1(a). The dual band FPA is composed by two different and interleaved sets of detectors [3]: the ones centered at 250 GHz, FSA_1, and ones centered at 500 GHz, FSA_2, as shown in Fig. 1(b).

In order to optimize the performance of an imager based on a focal plane array of FSAs, a spectral Fourier optics (FO) technique as described in [4] is used. The quasi-optical system of the imager consists of the dual lens focusing in the near field as described in [5].

II. POINT SPREAD FUNCTION OF THE IMAGING SYSTEM

The point spread function (PSF) of an imager represents the received power as a function of the position of the point source in the field of view (FoV). In this section, the experimental performance of the imager in terms of its effective PSF when coupled to a black body point source over a wide frequency band (100 GHz to 600 GHz) is reported. The two band pass filter stages, located in the instrument box (Fig. 1 (c)), determine this frequency band of operation.

This effective PSF was measured for two detectors (one per each bandwidth) at a distance from the center of the FPA, $\rho_{det} = 31\,mm$ using the setup shown in Fig. 1(c). The measurement was performed by laterally displacing the black body point source in the FoV. The power received by the detectors is then measured through the KIDs read-out response.

The imager performance is estimated using the spectral analysis technique presented in [4]. In the current geometry, the dual lens structure is analyzed using the commercial software GRASP to derive the plane wave spectrum (PWS) generated by the optical system. As described in [4], the coupling mechanism between this PWS and the absorber can be represented via an equivalent Floquet circuit, Fig. 2. The periodic absorbing FSA response to a plane wave is included in the circuit via an equivalent admittance matrix, $\bar{Y}_{abs}(\vec{k}_\rho)$, evaluated using CST MWS. The input voltage waves, $V_+^{TE/TM}$, in the equivalent Floquet circuit can be related to the PWS.

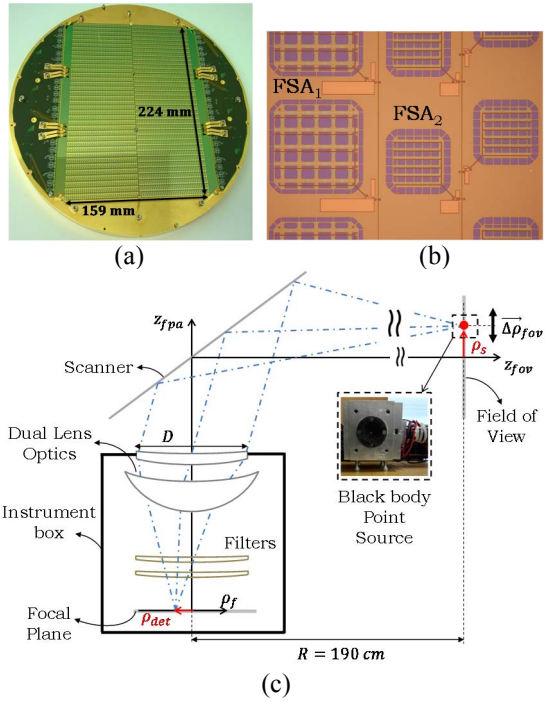

Fig. 1. (a) The dual band FPA. (b) The micrographic photos of the two FSA sets. (c) The schematic representation of the measurement setup of the imager.

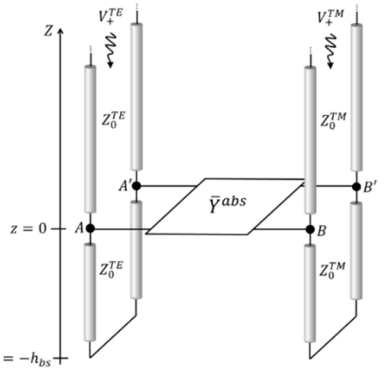

Fig. 2. The equivalent transmission line model of a periodic absorber with period smaller than half wavelength above a ground plane at distance h_{bs}.

One can follow the similar steps to the ones described in [4] to obtain the spatial fields representing the response of the absorber to the optical system, $\vec{e}^t(\vec{\rho}_f, \vec{\rho}_s)$ and $\vec{h}^t(\vec{\rho}_f, \vec{\rho}_s)$, where

the position of the source is explicitly indicated by $\vec{\rho}_s$. By integrating these fields, it is possible to calculate the power received by the imager as a function of the source position as:

$$P_{abs}(f,\vec{\rho}_s) \simeq \frac{1}{2} Re\left\{\iint_{-w/2}^{w/2} \left[\vec{e}_t(\vec{\rho}_f\ ,\vec{\rho}_s) \times \vec{h}_t^*(\vec{\rho}_f\ ,\vec{\rho}_s)\right] \cdot \hat{z}\, d\vec{\rho}\right\} \quad (1)$$

By normalizing the power received at broadside, $P_{abs}(f,\vec{\rho}_s)$, by the Poynting vector incident on the optical aperture, $S_{in}(\vec{\rho}_s)$, we can derive the effective area of the imager as

$$A_{eff}(f) = \frac{P_{abs}(f,\vec{\rho}_s)}{|S_{in}(\vec{\rho}_s)|} \quad (2)$$

and from that, the aperture efficiency can be calculated as

$$\eta_{ap}(f) \simeq \eta_{filt}^1(f)\eta_{filt}^2(f)\frac{A_{eff}(f)}{A_{ph}} \quad (3)$$

where A_{ph} is the physical area of the imager, η_{filt}^1 and η_{filt}^2 are the frequency response of the two filter stages. The aperture efficiencies for the two detectors are shown in Fig. 3. The maximum efficiency is approximately 20% in both bandwidths and the results for the two polarizations are comparable. This aperture efficiency includes the spillover associated to the diffracted fields in the focal plane, the ohmic and reflection losses of the dual-lens, the response of the two filter stages, and the frequency response of the FSAs. Moreover, a full wave simulation is performed to validate this efficiency. The efficiency obtained using the full wave simulation is also reported in Fig. 3.

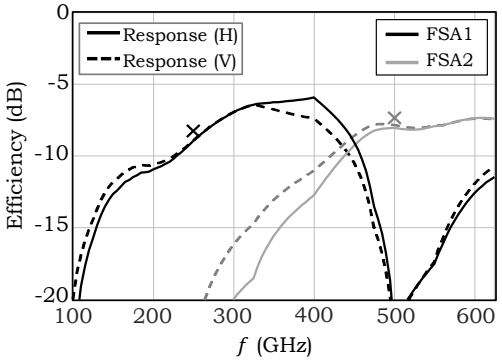

Fig. 3. The aperture efficiency of the two FSA sets (FSA_1 with side length 1.5 mm and FSA_2 with side length 0.9 mm). The cross marks represent the results obtained using the full wave simulations for horizontal polarization

In the following, the response of the imager to an incoherent point source, radiating over the whole frequency band ($BW =$ 100 to 625 GHz), is evaluated. The quality of an image is indeed dictated by the power received over the whole bandwidth. This effective PSF is estimated in the Rayleigh Jean's limit, for a black body point source with an average temperature distribution, and for two detectors (one per each bandwidth) at a distance from the center of the FPA, Fig. 1(c). The results are shown in Fig. 4 for FSA_1 and FSA_2 and compared to the theoretical computation based on the spectral Fourier optics methodology. The theory and the experiments are in excellent agreement until $-10\ dB$. Below this value, the noise due to the measurement setup is dominant. The pattern shows good symmetry, and its half power beam width (HPBW) is comparable to the diffraction limited HPBW.

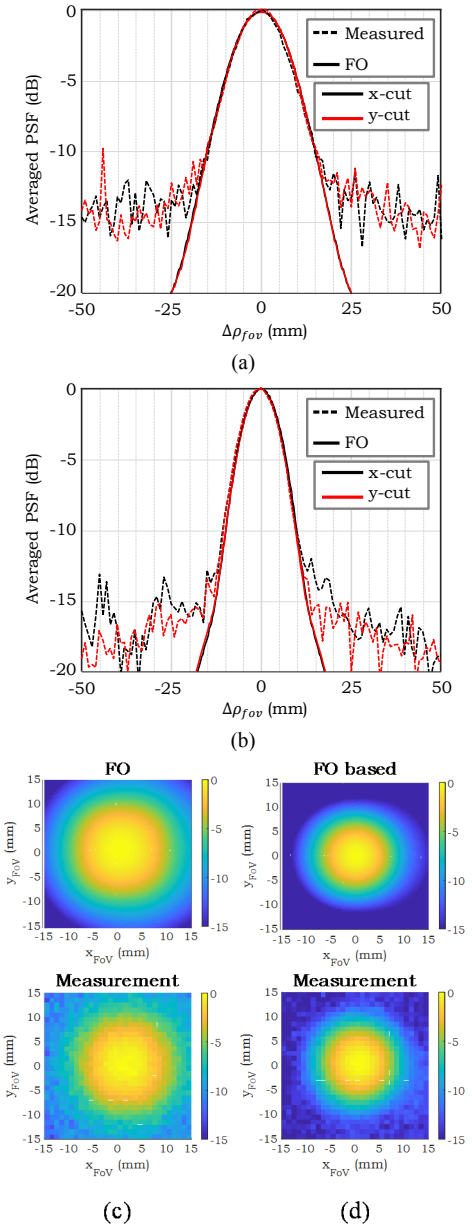

Fig. 4. The normalized effective point spread function compared between the proposed method and the measurement of (a) FSA_1 and (b) FSA_2 for vertical polarization. The 2D version of the same patterns are shown in (c) for FSA_1 and (d) for FSA_2.

Acknowledgment

This work was supported by ERC Starting Grant (ERC-2014-StG LAA-THz-CC), No. 639749 and FP7-Security project CONSORTIS

References

[1]. R. Appleby and H. Wallace, "Standoff detection of weapons and contraband in the 100 GHz to 1 THz region," *IEEE TAP*, 2007.

[2]. A. V. Timofeev, et al., "Submillimeter-wave kinetic inductance bolometers on free-standing nanomembranes," *SST*, vol. 27, no. 2, 2014

[3]. S. O. Dabironezare, et al., "Optimization of Frequency Selective Absorbers for Sub-mm Security Imagers", *IRMMW-THz*, Copenhagen, Denmark, 2016.

[4]. N. Llombart, et. al, "Fourier optics analysis of focal plane arrays of distributed absorbers: skew incidence," *IEEE TAP*, under review.

[5]. E. Gandini, et al., "Wide field of view inversely magnified dual-lens for near-field sub-millimeter wavelength imagers," *IEEE TAP*, vol. 66, no. 2, pp. 541-549, 2018.